



Classical threshold law for the formation of van der Waals molecules

Cite as: J. Chem. Phys. **155**, 094306 (2021); <https://doi.org/10.1063/5.0062812>

Submitted: 08 July 2021 . Accepted: 17 August 2021 . Published Online: 03 September 2021

 Marjan Mirahmadi, and  Jesús Pérez-Ríos



View Online



Export Citation



CrossMark

ARTICLES YOU MAY BE INTERESTED IN

[Reconsidering power functional theory](#)

The Journal of Chemical Physics **155**, 094901 (2021); <https://doi.org/10.1063/5.0055288>

[Software for the frontiers of quantum chemistry: An overview of developments in the Q-Chem 5 package](#)

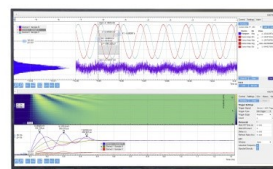
The Journal of Chemical Physics **155**, 084801 (2021); <https://doi.org/10.1063/5.0055522>

[Quantum dynamics with ab initio potentials](#)

The Journal of Chemical Physics **155**, 080401 (2021); <https://doi.org/10.1063/5.0066234>

Challenge us.

What are your needs for
periodic signal detection?



Zurich
Instruments



Classical threshold law for the formation of van der Waals molecules

Cite as: J. Chem. Phys. 155, 094306 (2021); doi: 10.1063/5.0062812

Submitted: 8 July 2021 • Accepted: 17 August 2021 •

Published Online: 3 September 2021



View Online



Export Citation



CrossMark

Marjan Mirahmadi  and Jesús Pérez-Ríos ^{a)} 

AFFILIATIONS

Fritz-Haber-Institut der Max-Planck-Gesellschaft, Faradayweg 4-6, D-14195 Berlin, Germany

^{a)} Author to whom correspondence should be addressed: jperezri@fhi-berlin.mpg.de

ABSTRACT

We study the role of pairwise long-range interactions in the formation of van der Waals molecules through direct three-body recombination processes $A + B + B \rightarrow AB + B$, based on a classical trajectory method in hyperspherical coordinates developed in our earlier works [J. Pérez-Ríos *et al.*, J. Chem. Phys. **140**, 044307 (2014); M. Mirahmadi and J. Pérez-Ríos, J. Chem. Phys. **154**, 034305 (2021)]. In particular, we find the effective long-range potential in hyperspherical coordinates with an exact expression in terms of dispersion coefficients of pairwise potentials. Exploiting this relation, we derive a classical threshold law for the total cross section and the three-body recombination rate yielding an analytical expression for the three-body recombination rate as a function of the pairwise long-range coefficients of the involved partners.

© 2021 Author(s). All article content, except where otherwise noted, is licensed under a Creative Commons Attribution (CC BY) license (<http://creativecommons.org/licenses/by/4.0/>). <https://doi.org/10.1063/5.0062812>

I. INTRODUCTION

van der Waals (vdW) molecules consist of two atoms held together by the long-range dispersion interaction¹ leading to (ground state) binding energies $\lesssim 1$ meV. Thus, setting aside ultralong-range Rydberg molecules (with binding energies ~ 4 neV²⁻⁶), vdW molecules show the weakest gas-phase molecular bond in nature. The binding mechanism in vdW molecules is the result of the compensation between the short-range repulsion, due to the overlap of closed-shell orbitals, and the attractive vdW interaction ($-C_6/r^6$) caused by zero point fluctuations of atomic dipole moments.

The study of vdW interactions provides a deeper understanding of crucial phenomena in physics, chemistry, and biology. For instance, these interactions play a key role in the formation and stability of gases, liquids, vdW heterostructures, and biopolymers;⁷⁻⁹ chemical reactions;¹⁰⁻¹³ superfluidity of ⁴He nanodroplets;^{14,15} and rare gas crystals and the dynamics of impurities interacting with dense rare gas vapors.^{16,17}

Recent developments in cooling techniques, specifically buffer gas cooling,¹⁸ have paved the way to new possibilities for investigating the formation of vdW molecules through three-body recombination processes.^{17,19-24} Three-body recombination is a three-body collision during which two of the particles form a bound state. These reactions play an important role in a wide range of physical and chemical phenomena, ranging from H₂ formation

in star-forming regions^{25,26} to loss mechanisms in ultracold dilute atomic gases²⁷⁻³³ to the formation and trapping of cold and ultracold molecules.³⁴⁻³⁸

In Ref. 39, we considered the formation of atom-rare gas vdW molecules via a direct three-body recombination mechanism at temperatures relevant for buffer gas cell experiments. As a result, we found that almost any atom in helium buffer gas will evolve into a vdW molecule. Fueled by those results, our goal in the present work is to present a comprehensive study of $A + B + B$ reactions and derive a classical threshold law for the formation of vdW molecules in cold environments. To investigate this problem, we use a classical approach in hyperspherical coordinates, which has previously been used to consider the three-body recombination of three neutral atoms,^{33,39,40} as well as ion-neutral-neutral three-body recombination processes.^{36,37,41} In order to derive a threshold law, we have obtained an effective long-range potential in hyperspherical coordinates. With this, a general expression (as a function of C_6^{AB} and $C_6^{B_2}$) for the corresponding dispersion coefficient is given by considering several A and B atoms chosen from alkali metals, alkaline-earth metals, transition metals, pnictogens, chalcogens, halogens, and rare gases. Furthermore, we calculated the threshold values for the three-body recombination rates at 4 K. Our results confirm that any vdW molecule AB appears with almost the same probability.

This paper is organized as follows: In Sec. II, the Hamiltonian governing the classical dynamics during three-body

recombination in the three-dimensional space and its counterpart in the six-dimensional space are introduced. In Sec. III, the long-range potential in hyperspherical coordinates has been obtained, and the relevant, effective dispersion coefficient as a function of dispersion coefficients of the pairwise interactions is found. In Sec. IV, a classical threshold law à la Langevin for the total cross section and the three-body recombination rate are developed. Finally, in Sec. V, we summarize our chief results and discuss their possible applications.

II. THREE-BODY RECOMBINATION IN HYPERSPHERICAL COORDINATES

Consider a system consisting of three particles with masses m_i ($i = 1, 2, 3$) at positions \vec{r}_i , interacting with each other via the potential $V(\vec{r}_1, \vec{r}_2, \vec{r}_3)$. The motion of these particles is governed by the Hamiltonian

$$H = \frac{\vec{p}_1^2}{2m_1} + \frac{\vec{p}_2^2}{2m_2} + \frac{\vec{p}_3^2}{2m_3} + V(\vec{r}_1, \vec{r}_2, \vec{r}_3), \quad (1)$$

with \vec{p}_i being the momentum vector of the i th particle. It is more convenient to treat the three-body problem in Jacobi coordinates^{42,43} defined by the following relations:

$$\begin{aligned} \vec{\rho}_1 &= \vec{r}_2 - \vec{r}_1, \\ \vec{\rho}_2 &= \vec{r}_3 - \vec{R}_{CM12}, \\ \vec{\rho}_{CM} &= \frac{m_1\vec{r}_1 + m_2\vec{r}_2 + m_3\vec{r}_3}{M}, \end{aligned} \quad (2)$$

where $\vec{R}_{CM12} = (m_1\vec{r}_1 + m_2\vec{r}_2)/(m_1 + m_2)$ is the center-of-mass vector of the two-body system consisting of m_1 and m_2 . $M = m_1 + m_2 + m_3$ and $\vec{\rho}_{CM}$ are the total mass and the center-of-mass vectors of the three-body system, respectively. The Jacobi vectors are illustrated in Fig. 1.

Due to conservation of the total linear momentum (i.e., $\vec{\rho}_{CM}$ is a cyclic coordinate), we omit the degrees of freedom of the center of

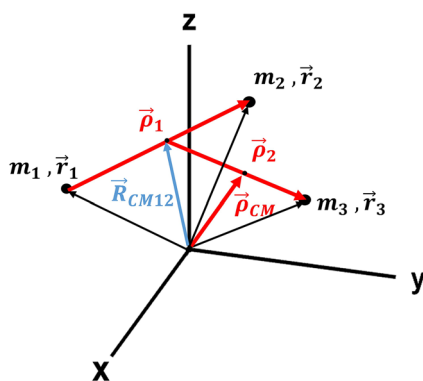


FIG. 1. Jacobi coordinates for the three-body problem illustrated by the red vectors. The black arrows indicate the position of the three particles in Cartesian coordinates, and the blue arrow indicates the two-body center-of-mass vector \vec{R}_{CM12} .

mass and write the Hamiltonian (1) as

$$H = \frac{\vec{P}_1^2}{2\mu_{12}} + \frac{\vec{P}_2^2}{2\mu_{3,12}} + V(\vec{\rho}_1, \vec{\rho}_2), \quad (3)$$

with reduced masses $\mu_{12} = m_1m_2/(m_1 + m_2)$ and $\mu_{3,12} = m_3(m_1 + m_2)/M$. Here, \vec{P}_1 and \vec{P}_2 indicate the conjugated momenta of $\vec{\rho}_1$ and $\vec{\rho}_2$, respectively. Note that, since the relations given by Eq. (2) indicate a canonical transformation, the Hamilton's equations of motion are invariant under the transformation to Jacobi coordinates.

A. Hyperspherical coordinates

In the next step, we map the independent relative coordinates of the three-body system associated with the Hamiltonian (3) in a three-dimensional (3D) space onto the degrees of freedom of a single particle moving toward a scattering center in a six-dimensional (6D) space under the effect of the Hamiltonian H^{6D} . This 6D space is described by means of hyperspherical coordinates consisting of a hyper-radius R and five hyperangles α_j (with $j = 1, 2, 3, 4, 5$), where $0 \leq \alpha_1 < 2\pi$ and $0 \leq \alpha_j > 1 \leq \pi$.^{44,45} The components of a 6D vector $\vec{x} = (x_1, x_2, x_3, x_4, x_5, x_6)$ in hyperspherical coordinates are given by

$$\begin{aligned} x_1 &= R \sin(\alpha_1) \sin(\alpha_2) \sin(\alpha_3) \sin(\alpha_4) \sin(\alpha_5), \\ x_2 &= R \cos(\alpha_1) \sin(\alpha_2) \sin(\alpha_3) \sin(\alpha_4) \sin(\alpha_5), \\ x_3 &= R \cos(\alpha_2) \sin(\alpha_3) \sin(\alpha_4) \sin(\alpha_5), \\ x_4 &= R \cos(\alpha_3) \sin(\alpha_4) \sin(\alpha_5), \\ x_5 &= R \cos(\alpha_4) \sin(\alpha_5), \\ x_6 &= R \cos(\alpha_5), \end{aligned} \quad (4)$$

and the volume element in this coordinate system is given by

$$\begin{aligned} d\tau &= R^5 dR d\Omega \\ &= R^5 dR \prod_{j=1}^5 \sin^{j-1}(\alpha_j) d\alpha_j. \end{aligned} \quad (5)$$

The 6D position and momentum vectors can be constructed from the Jacobi vectors and their conjugated momenta as^{40,46}

$$\vec{\rho} = \begin{pmatrix} \vec{\rho}_1 \\ \vec{\rho}_2 \end{pmatrix} \quad (6)$$

and

$$\vec{P} = \begin{pmatrix} \sqrt{\frac{\mu}{\mu_{12}}} \vec{P}_1 \\ \sqrt{\frac{\mu}{\mu_{3,12}}} \vec{P}_2 \end{pmatrix}, \quad (7)$$

respectively. Here, $\mu = \sqrt{m_1m_2m_3}/M$ is the three-body reduced mass. Consequently, the Hamiltonian in the 6D space reads as

$$H^{6D} = \frac{\vec{P}^2}{2\mu} + V(\vec{\rho}). \quad (8)$$

B. Total cross section and three-body recombination rate

Classically, for scattering in a 3D space, the cross section σ is defined as the area drawn in a plane perpendicular to particle's

initial momentum, which the particle's trajectory should cross in order to be scattered (i.e., deviation from the uniform rectilinear motion). This concept can be extended to the 6D space by visualizing it as an area in a five-dimensional hyperplane (embedded in the 6D space) perpendicular to the initial momentum vector \vec{P}_0 . Similarly, we define the impact parameter vector \vec{b} as the projection of the initial position vector $\vec{\rho}_0$ on this hyperplane; thus, the necessary condition $\vec{b} \cdot \vec{P}_0 = 0$ is satisfied.⁴⁶

Note that by treating the three-body collision as a scattering problem of a single particle in a 6D space, we can uniquely define the initial conditions and the impact parameter. Hence, it is possible to obtain the probability of a three-body recombination event as a function of the impact parameter \vec{b} and the initial momentum \vec{P}_0 . Consequently, by averaging over different orientations of \vec{P}_0 and making use of its relation with the collision energy $E_c = P_0^2/(2\mu)$, the total cross section of the three-body recombination process will be given by

$$\begin{aligned} \sigma_{\text{rec}}(E_c) &= \int \mathcal{P}(E_c, \vec{b}) b^4 db d\Omega_b \\ &= \frac{8\pi^2}{3} \int_0^{b_{\text{max}}(E_c)} \mathcal{P}(E_c, b) b^4 db, \end{aligned} \quad (9)$$

with $d\Omega_b$ being the differential element of the solid hyperangle associated with the vector \vec{b} . To obtain the second equality, we made use of $\Omega_b = 8\pi^2/3$. The function \mathcal{P} in Eq. (9) is the so-called opacity function, i.e., the probability of a recombination event as a function of the impact parameter and collision energy. Note that b_{max} represents the largest impact parameter for which three-body recombination occurs, or in other words, $\mathcal{P}(E_c, b) = 0$ for $b > b_{\text{max}}$.

Finally, the energy-dependent three-body recombination rate can be achieved via the following relation:

$$k_3(E_c) = \sqrt{\frac{2E_c}{\mu}} \sigma_{\text{rec}}(E_c). \quad (10)$$

C. Potential

Throughout the present work, we make use of the pairwise-additive approximation, which states that the total potential of a N -body system is the sum of all two-body interactions in the system. Thus, introducing the pairwise potentials $U(r_{ij})$, where $r_{ij} = |\vec{r}_j - \vec{r}_i|$, we write the interaction potential V in Eq. (1) in the following form:

$$V(\vec{r}_1, \vec{r}_2, \vec{r}_3) = U(r_{12}) + U(r_{23}) + U(r_{31}). \quad (11)$$

It is known that the pairwise-additive descriptions of vdW interactions provide appropriate results for the calculation of crystal binding energies⁴⁷ (showing deviations $\lesssim 10\%$), long-range coefficients of small molecules,⁴⁸ and the spectroscopy of clusters,⁴⁹ although in the latter case it is used only for its convenience. However, there are some scenarios in which a many-body interaction term is required, namely, the calculation of long-range coefficients in large molecules⁴⁸ and accurate spectroscopic constants of vdW complexes.⁴⁷ On the contrary, scattering observables are accurately described at the ultracold limit without invoking many-body interaction terms in the underlying potential energy surface (see, e.g., Ref. 50). Based on these examples and considering the nature of

systems studied in this work, a pairwise approximation for the three-body potential $V(\vec{r}_1, \vec{r}_2, \vec{r}_3)$ is convenient.

The relative distances r_{ij} in the Cartesian coordinate are related to the Jacobi vectors through the following equations:

$$\begin{aligned} r_{12} &= |\vec{\rho}_1|, \\ r_{23} &= \left| \vec{\rho}_2 - \frac{m_1}{m_1 + m_2} \vec{\rho}_1 \right|, \\ r_{31} &= \left| \vec{\rho}_2 + \frac{m_2}{m_1 + m_2} \vec{\rho}_1 \right|. \end{aligned} \quad (12)$$

Using these relations together with Eq. (6), we can obtain the potential $V(\vec{\rho})$ in Eq. (8) from Eq. (11). It is important to emphasize that, due to the relations given by Eq. (4), the potential is a function of the magnitude of the 6D position vector, ρ , and the corresponding hyperangles $\alpha \equiv (\alpha_1, \alpha_2, \alpha_3, \alpha_4, \alpha_5)$; in other words, $V(\vec{\rho}) \equiv V(\rho, \alpha)$.

D. Grand angular momentum

To finalize this section, let us briefly explain the notion of grand angular momentum in hyperspherical coordinates. Further below, we will use this discussion to develop a capture model in the hyperspherical coordinate system and with it a classical threshold law, which is the main purpose of this work. In classical mechanics, angular momentum in 6D space is a bivector defined by the exterior product (also known as the wedge product) of the 6D position and momentum vectors as

$$\Lambda = \vec{\rho} \wedge \vec{P}, \quad (13)$$

which is isomorphic to a 6×6 skew-symmetric matrix with elements

$$\Lambda_{ij} = \rho_i P_j - \rho_j P_i, \quad (14)$$

for $i, j = 1, 2, \dots, 6$. This general definition applies in all higher-dimensional spaces, and for the 3D space, it coincides with the familiar cross product. It is worth mentioning that even though Λ is not equal to the ordinary total angular momentum of the three-body system in the 3D space, it contains the components of the angular momenta (associated with Jacobi vectors) among its elements. Following the original definition by Smith in Ref. 51, Λ is often referred to as the grand angular momentum.

Note that in quantum mechanics, Λ is an operator. Its square, Λ^2 , is the quadratic Casimir operator of $\text{so}(6)$ with eigenvalues $\lambda(\lambda + 4)$, where λ is a positive integer, and with hyperspherical harmonics as the corresponding eigenfunctions.^{45,52,53}

III. LONG-RANGE POTENTIAL IN HYPERSPHERICAL COORDINATES

Consider a three-body collision $A + B + B$, where A and B are neutral atoms in their ground electronic state. The interaction potential $U(r_{ij})$ consists of a short-range repulsive interaction (due to the overlap of closed-shell orbitals) and a long-range vdW tail,

$$U(r_{ij}) \rightarrow -\frac{C_6}{r_{ij}^6}, \quad (15)$$

for r_{ij} greater than the LeRoy radius.

In Ref. 39, we have shown that the formation of vdW molecules through direct three-body recombination at collision energies lower

than the dissociation energy of the product molecule ($E_c < D_c^{AB}$) is insensitive to the short-range interaction and is dominated by the long-range tail of the potential. Note that we do not consider the contribution of higher order terms ($1/r^8, 1/r^{10}, \dots$) in the long-range tail of the potential since the effect of long-range interactions on formation of vdW complexes is mainly through the $1/r^6$ term.³⁹ Our goal is to find a general expression for the long-range interaction potential associated with the three-body collision A + B + B in a 6D space relevant for the classical trajectory method that we employ (see Fig. 2).

Following the discussion in Sec. II C, the long-range potential in hyperspherical coordinates is obtained via the relation

$$V_{LR}(\rho, \alpha) = -\frac{C_6^{B_2}}{r_{12}^6} - \frac{C_6^{AB}}{r_{23}^6} - \frac{C_6^{AB}}{r_{31}^6}. \quad (16)$$

To fix the coefficients in this equation, we made use of different atoms chosen from alkali metals, alkaline-earth metals, transition metals, pnictogens, chalcogens, halogens, and rare gases. These atoms together with the dispersion coefficients of the pairwise interactions between atoms A and B, C_6^{AB} , and between two B atoms, $C_6^{B_2}$, are listed in Table I.

A. ρ -distribution

To find the radial dependence of the potential $V_{LR}(\rho, \alpha)$, referred to as $V_{LR}(\rho)$ in Fig. 2, we set the right-hand side of Eq. (16) equal to a constant, $-Q$, and solve the equation,

$$\frac{C_6^{B_2}}{r_{12}^6(\rho, \alpha)} + \frac{C_6^{AB}}{r_{23}^6(\rho, \alpha)} + \frac{C_6^{AB}}{r_{31}^6(\rho, \alpha)} = Q, \quad (17)$$

for randomly sampled hyperangles. Different hyperangles α_j are generated by means of the probability density function associated with $d\Omega$ given in Eq. (5) to generate random points uniformly distributed on the six-sphere (in the geometrical sense). This procedure implies that the solution of Eq. (17) will be obtained as a distribution of ρ values, $f(\rho)$, for each particular Q . Finally, we choose $\rho = \rho_m$ with the maximum likelihood in the ρ -distribution, as a single value solution of Eq. (17). We select Q from interval [0.001, 1000] K and solve the equation for 10^4 randomly generated sets of hyperangles. Note that even though for each set of α , Eq. (17) will be transformed into a sixth-degree equation of the variable ρ , we have seen that

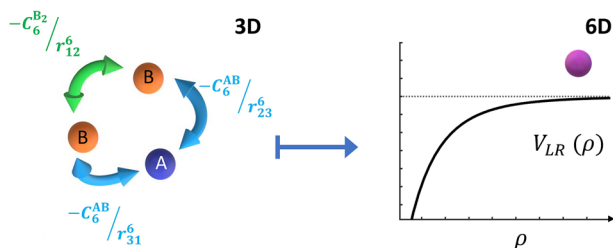


FIG. 2. A schematic illustration of the long-range vdW interaction between three particles in 3D space and its counterpart, $V_{LR}(\rho)$, for a single particle in the 6D space.

(regardless the value of Q) four of the roots are complex, and from the two remaining real roots, only one is positive.

Interestingly enough, for all chosen values of Q and dispersion coefficients, the probability density function (PDF) of the ρ -distribution, $F_f(\rho)$, is described by the PDF of the generalized extreme value (GEV) distribution, i.e.,

$$F_f(\rho) = \frac{1}{\delta} \exp \left[- \left(1 + \xi \frac{\rho - \beta}{\delta} \right)^{-\frac{1}{\xi}} \right] \left(1 + \xi \frac{\rho - \beta}{\delta} \right)^{-1 - \frac{1}{\xi}}, \quad (18)$$

with $1 + \xi \frac{\rho - \beta}{\delta} > 0$. The GEV distribution is a family of continuous probability distributions developed within the extreme value theory.^{65,66} It is parameterized with a shape parameter $\xi \neq 0$, a location parameter β , and a scale parameter δ . It is worth mentioning that here $\xi > 0$, which corresponds to type II (also known as the Fréchet distribution) of GEV distributions.⁶⁶ The parameters of GEV in Eq. (18) are fitted, yielding an uncertainty below 0.05%.

As an illustration, the distribution $f(\rho)$ obtained by setting $Q = 1$ mK in Eq. (17) for the three-body collision As + He + He is shown in Fig. 3. As can be seen in Fig. 3, the probability density is positively skewed. Therefore, due to this skewness, the maximum ρ_m is achieved by using the mode of the GEV distribution,

$$\rho_m = \beta + \frac{\delta}{\xi} \left((1 + \xi)^{-\xi} - 1 \right), \quad (19)$$

instead of its mean value.

It is worth mentioning that we have observed the same (hyper)radial distribution $f(\rho)$ also in the case of pairwise interactions proportional to $1/r^4$. In other words, if we change an atom by an ion, the distribution of the hyper-radius ρ is of the same kind. However, the results of such a study are beyond the scope of this work and will be considered elsewhere.

B. Effective dispersion coefficient

The general form of the long-range potential $V_{LR}(\rho)$ in the 6D space can be derived from the power-law relation between Q and $\rho (= \rho_m)$. An example has been shown in Fig. 4. It can be seen that, as expected, Q is proportional to $1/\rho^6$ and the corresponding effective dispersion coefficient, C_{eff} , is the slope of the fitted line in the log-log scale. Therefore, C_{eff} can be obtained as a function of C_6^{AB} and $C_6^{B_2}$ of the pairwise vdW interactions. Finally, utilizing Eqs. (16) and (17), we have

$$V_{LR}(\rho) = -\frac{C_{\text{eff}}}{\rho^6}. \quad (20)$$

Through the same procedure for all A-B-B systems mentioned in Table I and calculating the corresponding vdW coefficients C_{eff} , we have found the general expression

$$C_{\text{eff}} = a(C_6^{AB})^c + d(C_6^{B_2})^g, \quad (21)$$

with parameters $a = 0.56 \pm 0.04$, $c = 0.189 \pm 0.009$, $d = 1.19 \pm 0.04$, and $g = 0.155 \pm 0.003$. Equation (21) is applicable to any three-body system leading to the formation of vdW molecules. Note that C_{eff} is in atomic units, and the value of parameters a, b, c , and

TABLE I. Dispersion coefficients of pairwise potentials contributing in different three-body collisions $A + B + B$ and their corresponding temperature-dependent three-body recombination rates calculated from Eq. (28) at $T = 4$ K, a relevant temperature for buffer gas cell experiments. All the dispersion coefficients are given in atomic units, and $k_3(T)$ is given in units of cm^6/s .

A-B-B	C_6^{AB}	$C_6^{\text{B}_2}$	$k_3(T = 4 \text{ K}) (\times 10^{-32})$	A-B-B	C_6^{AB}	$C_6^{\text{B}_2}$	$k_3(T = 4 \text{ K}) (\times 10^{-32})$
Li-He-He	22.51 ^a	1.35 ^a	2.99	F-Ar-Ar	33.44 ^b	64.3	1.64
Na-	23.77 ^a		2.67	Cd-	173.6 ^c		1.36
K-	39.47 ^d		2.69	Hg-	129.9 ^c		1.28
Be-	12.98 ^e		2.79	Zn-	139.4 ^c		1.44
Ca-	36.59 ^d		2.68	Li-Kr-Kr	255 ^e	129.6 ^e	1.99
Sr-	38.64 ^f		2.62	Na-	289 ^e		1.53
N-	5.7 ^f		2.53	K-	444.2 ^d		1.40
O-	5.83 ^b		2.50	Be-	146 ^e		1.82
As-	17.16 ^f		2.49	Ca-	400 ^e		1.39
P-	14.69 ^f		2.54	Sr-	482.1 ^d		1.21
Ti-	27.61 ^a		2.60	O-	64.77 ^b		1.52
Cd-	24.93 ^c		2.53	F-	47.53 ^b		1.44
Hg-	18.92 ^c		2.46	Cd-	250.9 ^c		1.12
Zn-	20.1 ^c		2.52	Hg-	186.9 ^c		1.02
Li-Ne-Ne	46.4 ^e	6.38 ^e	2.09	Zn-	201.2 ^c		1.21
Na-	52.4 ^e		1.69	Li-Xe-Xe	404 ^e	285.9 ^e	1.94
K-	77.5 ^d		1.61	Na-	460.8 ^d		1.48
Be-	27.7 ^e		1.92	K-	698.1 ^d		1.35
Ca-	74.8 ^e		1.60	Be-	226 ^e		1.77
Sr-	86.36 ^d		1.49	Ca-	624 ^e		1.33
O-	13.13 ^b		1.64	Sr-	750.3 ^d		1.14
Cd-	46.3 ^c		1.40	O-	103.4 ^b		1.48
Hg-	34.99 ^c		1.34	F-	79.4 ^b		1.40
Zn-	37.29 ^c		1.45	Cd-	385.7 ^c		1.05
Li-Ar-Ar	174.1 ^d	64.3 ^e	2.24	Hg-	285.8 ^c		0.94
Na-	196.8 ^d		1.75	Zn-	308.9 ^c		1.15
K-	317 ^e		1.64	Be-Li-Li	467 ^e	1389 ^e	4.91
Be-	101 ^e		2.05	Be-Na-Na	522 ^d	1363 ^e	3.39
Ca-	276 ^e		1.62	Be-Mg-Mg	364.9 ^d	629.6 ^d	3.07
Sr-	327.1 ^d		1.46	Be-Be-Be	213 ^e	213	3.69
O-	43.88 ^b		1.73	He-He-He	1.35 ^a	1.35	2.74

^aDispersion coefficient C_6 for alkali-helium pairs is taken from Refs. 54 and 55, for He-He from Ref. 56, and for Ti-He from Ref. 39.

^bDispersion coefficient C_6 for O-B is taken from Ref. 63 and for F-B from Ref. 64.

^cDispersion coefficient C_6 is obtained through the London-Drude theory of dispersion interactions and taken from Ref. 8.

^dDispersion coefficient C_6 is taken from Ref. 57.

^eThe dispersion coefficient C_6 is taken from Refs. 58-60.

^fDispersion coefficient C_6 for Sr-B is taken from Ref. 61 and for pnictogen-He from Ref. 62.

d should be modified for C_{eff} in other systems of units. Figure 5 displays the surface plot of the coefficients obtained from Eq. (21) with the mentioned parameters, plotted for different values of C_6^{AB} and $C_6^{\text{B}_2}$.

IV. CLASSICAL THRESHOLD LAW

A threshold law for the three-body recombination cross section and rate can be established based on the pioneering capture theory of Langevin.⁶⁷ In the framework of this classical capture model, every trajectory associated with the collision energy (E_c) above the potential barrier leads, with unit probability, to a reaction event. To

implement the same idea in the 6D space, we first need to define the effective potential.

In a three-body collision, after including the centrifugal energy, the effective long-range potential in hyperspherical coordinates reads as⁵¹ (in atomic units)

$$V_{\text{eff}}(\rho) = V_{\text{LR}}(\rho) + \frac{\Lambda^2}{2\mu\rho^2}, \quad (22)$$

with a maximum (the so-called centrifugal barrier) at $\rho_0 = (6\mu C_{\text{eff}}/\Lambda^2)^{1/4}$. Here, $\Lambda^2 = (\vec{p} \wedge \vec{P})^2$ can be obtained from the components given by Eq. (14), and after applying (algebraic)

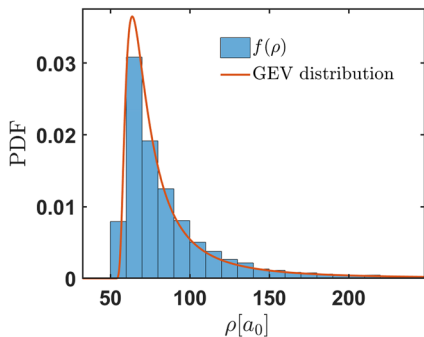


FIG. 3. The PDF of ρ -distribution $f(\rho)$ (blue histogram) and the fitted PDF of GEV distribution (red curve) for $Q = 1$ mK in the three-body collision As + He + He. ρ is given in units of the Bohr radius $a_0 \approx 5.29 \times 10^{-11}$ m. Parameters of GEV are obtained as $\xi \approx 0.67$, $\delta \approx 12.11$, and $\beta \approx 69.03$.

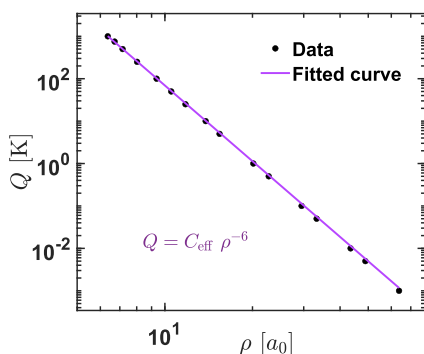


FIG. 4. Power-law relation between different Q and ρ values (circles) for the three-body recombination process As + He + He \rightarrow AsHe + He fitted with $Q = a\rho^b$ (purple line). The results are shown in the log–log scale.

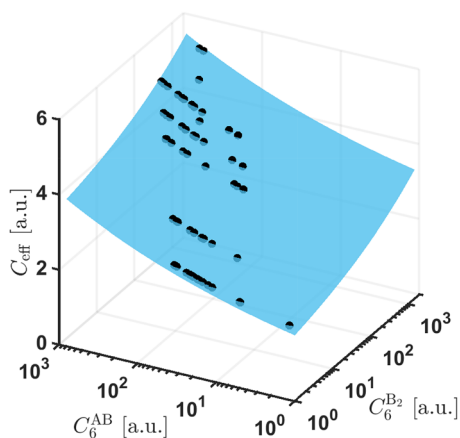


FIG. 5. Calculated effective dispersion coefficient C_{eff} for different A + B + B collisions shown in Table I (black symbols) together with C_{eff} calculated from Eq. (21) (blue surface). Note that the X and Y axis are in the logarithmic scale.

Lagrange's identity,⁶⁸ one finds

$$\begin{aligned} \Lambda^2 &\equiv \sum_{1 \leq i < j \leq 6} \Lambda_{ij}^2 = \left(\sum_{i=1}^6 \rho_i^2 \right) \left(\sum_{i=1}^6 P_i^2 \right) - \left(\sum_{i=1}^6 \rho_i P_i \right)^2 \\ &= \rho^2 P^2 - (\vec{\rho} \cdot \vec{P})^2. \end{aligned} \quad (23)$$

Utilizing the relation between the impact parameter vector \vec{b} and the initial position and momentum vectors,⁴⁰ we have $\vec{\rho}_0 \wedge \vec{P}_0 = \vec{b} \wedge \vec{P}_0$, where we used the fact that $\vec{P}_0 \wedge \vec{P}_0 = 0$. Finally, taking into account that $\vec{b} \perp \vec{P}_0$, one finds

$$\begin{aligned} \Lambda^2 &= (\vec{b} \wedge \vec{P}_0)^2 \\ &= b^2 P_0^2 - (\vec{b} \cdot \vec{P}_0)^2 \\ &= 2\mu E_c b^2, \end{aligned} \quad (24)$$

which establishes the intimate relation between the grand angular momentum and the magnitude of the impact parameter.

Knowing that a reaction occurs only if $E_c \sim V_{\text{eff}}(\rho_0)$, we can find a threshold value for the impact parameter, b_{max} , which is assigned to $E_c = V_{\text{eff}}(\rho_0)$. Upon substituting for Λ^2 obtained from Eq. (24) into $V_{\text{eff}}(\rho_0)$, we derive the relation

$$b_{\text{max}} = \sqrt{\frac{3}{2}} \left(\frac{2C_{\text{eff}}}{E_c} \right)^{1/6}. \quad (25)$$

Inserting Eq. (25) into Eq. (9), we obtain the geometric cross section ($\mathcal{P}(E_c, b) = 1$ for $b \leq b_{\text{max}}$) in the following form:

$$\begin{aligned} \sigma_{\text{rec}}(E_c) &= \frac{8\pi^2}{3} \int_0^{b_{\text{max}}(E_c)} b^4 db \\ &= \frac{6\sqrt{3}\pi^2}{5\sqrt{2}} (2C_{\text{eff}})^{5/6} E_c^{-5/6} \\ &= \frac{6\sqrt{3}\pi^2}{5\sqrt{2}} \left[2a(C_6^{\text{AB}})^c + 2d(C_6^{\text{B}_2})^g \right]^{5/6} E_c^{-5/6}, \end{aligned} \quad (26)$$

where in the last line we made use of Eq. (21). Employing Eq. (10), the three-body recombination rate can be calculated as a function of the collision energy and dispersion coefficients of the pairwise interactions as

$$k_3(E_c) = \frac{6\sqrt{3}\pi^2}{5\sqrt{\mu}} \left[2a(C_6^{\text{AB}})^c + 2d(C_6^{\text{B}_2})^g \right]^{5/6} E_c^{-1/3}. \quad (27)$$

Finally, the corresponding thermal average is obtained via integrating Eq. (27) over the appropriate three-body Maxwell–Boltzmann distribution of collision energies, yielding

$$\begin{aligned} k_3(T) &= \frac{1}{2(k_B T)^3} \int_0^\infty k_3(E_c) E_c^2 e^{-E_c/(k_B T)} dE_c, \\ &= \frac{4\pi^3 (k_B T)^{-1/3}}{3\Gamma(1/3)\sqrt{\mu}} \left[2a(C_6^{\text{AB}})^c + 2d(C_6^{\text{B}_2})^g \right]^{5/6}, \end{aligned} \quad (28)$$

where k_B is the Boltzmann constant and $\Gamma(x)$ is the gamma function of argument x . We should emphasize that these relations are best valid for collision energies smaller than the dissociation energy

of the vdW molecules, which is typically below 100 K (≈ 10 meV). Moreover, one should also verify the validity of the classical approach based on the number of involving partial waves, which will be discussed in what follows.

A. Estimated number of contributing three-body partial waves

From the perspective of a scattering problem of a single particle in a 6D space, each (grand) angular momentum quantum number λ is a so-called partial wave. Following this fact, we introduce λ as the partial wave associated with a three-body recombination in 3D space.

It is known that the reliability of the classical approach depends on the number of partial waves contributing to the scattering observables.^{46,69} In other words, the large number of partial waves (≈ 20) contributing to the scattering washes out quantum effects, such as resonances. The number of partial waves that impart a significant effect to the scattering problem can be estimated from the strength of the interaction, i.e., the collision energy E_c .^{39,46}

Setting Λ^2 equal to the eigenvalues of its quantum mechanical counterpart, $\lambda(\lambda + 4)$, from $V_{\text{eff}}(\rho_0) = E_c$, we can establish the following relation between the maximum three-body partial wave λ_{max} and a given collision energy:

$$\lambda_{\text{max}} = \sqrt{6\mu} \left[a(C_6^{\text{AB}})^c + d(C_6^{\text{B}_2})^g \right]^{1/6} \left(\frac{E_c}{2} \right)^{1/3}, \quad (29)$$

where we made use of the fact that for $\lambda \gg 4$, $\lambda(\lambda + 4) \rightarrow \lambda^2$. Equation (29) provides a measure to check the validity of classical calculations for different A-B-B systems based on the collision energy, reduced mass, and pairwise dispersion coefficients. For a more detailed comparison between the quantum and classical results obtained by hyperspherical classical trajectory method in three-body recombination, see Ref. 40.

B. Low-energy limit: s-wave collisions

In the final part of this section, we derive a classical threshold law associated with the quantum s-wave scattering, i.e., $\lambda = 0$. In this case, one may define the parameter b_{max} as the distance at which the collision energy is comparable to the strength of the interaction potential, i.e., $E_c = C_6^{\text{B}_2} r_{12}^{-6} + C_6^{\text{AB}} r_{23}^{-6} + C_6^{\text{AB}} r_{31}^{-6}$ in the 3D space or equivalently $E_c = C_{\text{eff}} \rho^{-6}$ in the 6D space. Therefore, the maximum impact parameter in the hyperspherical coordinate system reads as

$$b_{\text{max}} = \left(\frac{C_{\text{eff}}}{E_c} \right)^{1/6}. \quad (30)$$

By a similar argument as above, we obtain the cross section from Eq. (9), which yields

$$\sigma_{\text{rec}}^{\text{sw}}(E_c) = \frac{8\pi^2}{15} \left[a(C_6^{\text{AB}})^c + d(C_6^{\text{B}_2})^g \right]^{5/6} E_c^{-5/6}. \quad (31)$$

Consequently, the three-body recombination $k_3^{\text{sw}}(E_c)$ and its thermal average $k_3^{\text{sw}}(T)$ are given by

$$k_3^{\text{sw}}(E_c) = \frac{8\sqrt{2}\pi^2}{15\sqrt{\mu}} \left[a(C_6^{\text{AB}})^c + d(C_6^{\text{B}_2})^g \right]^{5/6} E_c^{-1/3} \quad (32)$$

and

$$k_3^{\text{sw}}(T) = \frac{16\sqrt{2}\pi^3(k_B T)^{-1/3}}{27\Gamma(1/3)\sqrt{3}\mu} \left[a(C_6^{\text{AB}})^c + d(C_6^{\text{B}_2})^g \right]^{5/6}, \quad (33)$$

respectively.

C. Results

The results derived by performing the thermal average (28) for different A + B + B reactive collisions for $T = 4$ K (relevant for buffer gas cells) are shown in Table I. To calculate these values, we used the mass of the most abundant isotopes of A and B atoms. Note that the calculated recombination rates account for both AB and B₂ products of the three-body process. However, based on the relative values of the dispersion coefficients, AB molecules are formed more often than B₂ ones, unless the dispersion coefficient for B₂ is larger than that of AB. It is important to notice that all calculated three-body recombination rates are of the same order of magnitude. One reason is the very close values of C_{eff} obtained for different systems, which almost neutralizes the effect of the three-body reduced mass μ .

Table II shows the three-body recombination rates $k_3(T)$ given by Eq. (28) for six different A + He + He collisions at $T = 4$ K, together with values of $k_3^{\text{num}}(T)$ taken from Ref. 39. $k_3^{\text{num}}(T)$ are the numerical values calculated via the classical trajectory method introduced in Ref. 40. The recombination rates $\tilde{k}_3(T)$ in this table are obtained from a capture model that only takes into account the pairwise interaction of the stronger long-range tail, i.e.,³⁹

$$\tilde{k}_3(T) = \frac{4\pi^3(k_B T)^{-1/3}}{\Gamma(1/3)\sqrt{\mu}} (2C_6^{\text{AB}})^{5/6}. \quad (34)$$

It can be seen that the trend of the rates calculated with a capture model à la Langevin (k_3) is in reasonably good agreement with the trend of k_3^{num} except for Li and Na. This is because the dissociation energy of LiHe and NaHe is below 2 K. Hence, the collision energies considered to calculate $k_3(T = 4$ K) have reached the high-energy regime ($E_c > D_e$). Since this regime is sensitive to the short region of the potential, the capture model is not as accurate as in the other cases. Finally, we must highlight the considerable improvement (about one order of magnitude) in the threshold values k_3 obtained from Eq. (28) over those values derived from the threshold law given by Eq. (34).

TABLE II. Temperature-dependent three-body recombination rates $k_3(T)$ from Eq. (28), $\tilde{k}_3(T)$ from Eq. (34), and k_3^{num} from Ref. 39 calculated at $T = 4$ K. Recombination rates are given in units of ($\text{cm}^6/\text{s} \times 10^y$), where y is given in parentheses beside of each number.

A	k_3	\tilde{k}_3	k_3^{num}
Li	2.99 (−32)	2.03 (−31)	5.94 (−33)
Na	2.68 (−32)	1.89 (−31)	9.30 (−34)
N	2.53 (−32)	5.99 (−32)	3.00 (−33)
As	2.49 (−32)	1.37 (−31)	2.94 (−33)
P	2.54 (−32)	1.25 (−31)	3.09 (−33)
Ti	2.61 (−32)	2.07 (−31)	3.09 (−33)

V. CONCLUSIONS AND PROSPECTS

After developing a clear picture of the (hyper)radial dependence of a three-body potential in a 6D space and studying more than 40 three-body systems relevant for vdW molecule formation, we have found how the long-range interaction of three-body systems depends on pairwise interactions between the colliding partners. Then, employing a classical trajectory method in hyperspherical coordinates, we have established a classical threshold law for the formation of vdW molecules through direct three-body recombination processes relevant for buffer gas cooling experiments. In addition, we have shown that at a given temperature, the three-body recombination rate is of the same order of magnitude independently of the atomic species under consideration, which corroborates our previous studies on the matter.

The most valuable achievement of this work is to offer a simple expression that makes it possible to obtain the three-body recombination rate by only using the long-range dispersion coefficients and masses of the colliding atoms. This result helps to quickly estimate the role of three-body recombination in a given scenario and with it provides a new avenue for the calculation of three-body recombination rates avoiding costly computations. Finally, we hope that our findings help to make three-body collisions more approachable for the chemical physics community.

ACKNOWLEDGMENTS

We would like to thank Miruna T. Cretu for valuable discussions and Gerard Meijer for his support and interest.

DATA AVAILABILITY

The data that support the findings of this study are available from the corresponding author upon reasonable request.

REFERENCES

- 1 B. L. Blaney and G. E. Ewing, "Van Der Waals molecules," *Annu. Rev. Phys. Chem.* **27**, 553–584 (1976).
- 2 C. H. Greene, A. S. Dickinson, and H. R. Sadeghpour, "Creation of polar and nonpolar ultra-long-range Rydberg molecules," *Phys. Rev. Lett.* **85**, 2458–2461 (2000).
- 3 E. L. Hamilton, C. H. Greene, and H. R. Sadeghpour, "Shape-resonance-induced long-range molecular Rydberg states," *J. Phys. B* **35**, L199–L206 (2002).
- 4 V. Bendkowsky, B. Butscher, J. Nipper, J. P. Shaffer, R. Löw, and T. Pfau, "Observation of ultralong-range Rydberg molecules," *Nature* **458**, 1005–1008 (2009).
- 5 D. Booth, S. T. Rittenhouse, J. Yang, H. R. Sadeghpour, and J. P. Shaffer, "Production of trilobite Rydberg molecule dimers with kilo-Debye permanent electric dipole moments," *Science* **348**, 99–102 (2015).
- 6 T. Niederprüm, O. Thomas, T. Eichert, C. Lippe, J. Pérez-Ríos, C. H. Greene, and H. Ott, "Observation of pendular butterfly Rydberg molecules," *Nat. Commun.* **7**, 12820 (2016).
- 7 A. D. Buckingham, P. W. Fowler, and J. M. Hutson, "Theoretical studies of van der Waals molecules and intermolecular forces," *Chem. Rev.* **88**, 963–988 (1988).
- 8 J. Koperski, "Study of diatomic van der Waals complexes in supersonic beams," *Phys. Rep.* **369**, 177–326 (2002).
- 9 J. Hermann, R. A. DiStasio, and A. Tkatchenko, "First-principles models for van der Waals interactions in molecules and materials: Concepts, theory, and applications," *Chem. Rev.* **117**, 4714–4758 (2017).
- 10 R. E. Smalley, D. A. Auerbach, P. S. H. Fitch, D. H. Levy, and L. Wharton, "Laser spectroscopic measurement of weakly attractive interatomic potentials: The Na + Ar interaction," *J. Chem. Phys.* **66**, 3778–3785 (1977).
- 11 D. R. Worsnop, S. J. Buelow, and D. R. Herschbach, "Molecular beam study of van der Waals bond exchange in collisions of noble gas atoms and dimers," *J. Phys. Chem.* **90**, 5121–5130 (1986).
- 12 N. Balakrishnan, "On the role of van der Waals interaction in chemical reactions at low temperatures," *J. Chem. Phys.* **121**, 5563–5566 (2004).
- 13 Z. Shen, H. Ma, C. Zhang, M. Fu, Y. Wu, W. Bian, and J. Cao, "Dynamical importance of van der Waals saddle and excited potential surface in C(¹D) + D₂ complex-forming reaction," *Nat. Commun.* **8**, 14094 (2017).
- 14 J. P. Toennies and A. F. Vilesov, "Superfluid helium droplets: A uniquely cold nanomatrix for molecules and molecular complexes," *Angew. Chem., Int. Ed.* **43**, 2622–2648 (2004).
- 15 K. Szalewicz, "Interplay between theory and experiment in investigations of molecules embedded in superfluid helium nanodroplets," *Int. Rev. Phys. Chem.* **27**, 273–316 (2008).
- 16 I. Y. Fugol, "Excitons in rare-gas crystals," *Adv. Phys.* **27**, 1–87 (1978).
- 17 N. Brahms, T. V. Tschersbul, P. Zhang, J. Klos, R. C. Forrey, Y. S. Au, H. R. Sadeghpour, A. Dalgarno, J. M. Doyle, and T. G. Walker, "Formation and dynamics of van der Waals molecules in buffer-gas traps," *Phys. Chem. Chem. Phys.* **13**, 19125–19141 (2011).
- 18 R. DeCarvalho, J. M. Doyle, B. Friedrich, T. Guillet, J. Kim, D. Patterson, and J. D. Weinstein, "Buffer-gas loaded magnetic traps for atoms and molecules: A primer," *Eur. Phys. J. D* **7**, 289 (1999).
- 19 N. Brahms, B. Newman, C. Johnson, T. Greytak, D. Kleppner, and J. Doyle, "Magnetic trapping of silver and copper, and anomalous spin relaxation in the Ag-He system," *Phys. Rev. Lett.* **101**, 103002 (2008).
- 20 H. Suno and B. D. Esry, "Three-body recombination in cold helium–helium-alkali-metal-atom collisions," *Phys. Rev. A* **80**, 062702 (2009).
- 21 N. Brahms, T. V. Tschersbul, P. Zhang, J. Klos, H. R. Sadeghpour, A. Dalgarno, J. M. Doyle, and T. G. Walker, "Formation of van der Waals molecules in buffer-gas-cooled magnetic traps," *Phys. Rev. Lett.* **105**, 033001 (2010).
- 22 Y. Wang, J. P. D'Incao, and B. D. Esry, "Cold three-body collisions in hydrogen–hydrogen-alkali-metal atomic systems," *Phys. Rev. A* **83**, 1–9 (2011).
- 23 N. Tariq, N. A. Taisan, V. Singh, and J. D. Weinstein, "Spectroscopic detection of the LiHe molecule," *Phys. Rev. Lett.* **110**, 153201 (2013).
- 24 N. Quiros, N. Tariq, T. V. Tschersbul, J. Klos, and J. D. Weinstein, "Cold anisotropically interacting van der Waals molecule: TiHe," *Phys. Rev. Lett.* **118**, 213401 (2017).
- 25 D. R. Flower and G. J. Harris, "Three-body recombination of hydrogen during primordial star formation," *Mon. Not. R. Astron. Soc.* **377**, 705–710 (2007).
- 26 R. C. Forrey, "Rate of formation of hydrogen molecules by three-body recombination during primordial star formation," *Astrophys. J., Lett.* **773**, 2011–2013 (2013).
- 27 B. D. Esry, C. H. Greene, and J. P. Burke, "Recombination of three atoms in the ultracold limit," *Phys. Rev. Lett.* **83**, 1751–1754 (1999).
- 28 J. Weiner, V. S. Bagnato, S. Zilio, and P. S. Julienne, "Experiments and theory in cold and ultracold collisions," *Rev. Mod. Phys.* **71**, 1–85 (1999).
- 29 P. F. Bedaque, E. Braaten, and H.-W. Hammer, "Three-body recombination in Bose gases with large scattering length," *Phys. Rev. Lett.* **85**, 908–911 (2000).
- 30 H. Suno, B. D. Esry, and C. H. Greene, "Three-body recombination of cold fermionic atoms," *New J. Phys.* **5**, 53 (2003).
- 31 T. Weber, J. Herbig, M. Mark, H.-C. Nägerl, and R. Grimm, "Three-body recombination at large scattering lengths in an ultracold atomic gas," *Phys. Rev. Lett.* **91**, 123201 (2003).
- 32 M. Schmidt, H.-W. Hammer, and L. Platter, "Three-body losses of a polarized Fermi gas near a p-wave Feshbach resonance in effective field theory," *Phys. Rev. A* **101**, 062702 (2020).
- 33 C. H. Greene, P. Giannakeas, and J. Pérez-Ríos, "Universal few-body physics and cluster formation," *Rev. Mod. Phys.* **89**, 035006 (2017).
- 34 T. Köhler, K. Góral, and P. S. Julienne, "Production of cold molecules via magnetically tunable Feshbach resonances," *Rev. Mod. Phys.* **78**, 1311–1361 (2006).

- ³⁵D. Blume, “Few-body physics with ultracold atomic and molecular systems in traps,” *Rep. Prog. Phys.* **75**, 046401 (2012).
- ³⁶J. Pérez-Ríos and C. H. Greene, “Communication: Classical threshold law for ion-neutral-neutral three-body recombination,” *J. Chem. Phys.* **143**, 041105 (2015).
- ³⁷A. Krüchow, A. Mohammadi, A. Härter, J. H. Denschlag, J. Pérez-Ríos, and C. H. Greene, “Energy scaling of cold atom-atom-ion three-body recombination,” *Phys. Rev. Lett.* **116**, 193201 (2016).
- ³⁸A. Mohammadi, A. Krüchow, A. Mahdian, M. Deiß, J. Pérez-Ríos, H. da Silva, M. Raouf, O. Dulieu, and J. H. Denschlag, “Life and death of a cold BaRb⁺ molecule inside an ultracold cloud of Rb atoms,” *Phys. Rev. Res.* **3**, 013196 (2021).
- ³⁹M. Mirahmadi and J. Pérez-Ríos, “On the formation of van der Waals complexes through three-body recombination,” *J. Chem. Phys.* **154**, 034305 (2021).
- ⁴⁰J. Pérez-Ríos, S. Ragole, J. Wang, and C. H. Greene, “Comparison of classical and quantal calculations of helium three-body recombination,” *J. Chem. Phys.* **140**, 044307 (2014).
- ⁴¹J. Pérez-Ríos and C. H. Greene, “Universal temperature dependence of the ion-neutral-neutral three-body recombination rate,” *Phys. Rev. A* **98**, 23–26 (2018).
- ⁴²H. Pollard, *Celestial Mechanics* (American Mathematical Society, 1976).
- ⁴³Y. Suzuki, Y. Varga, M. Suzuki, and K. Varga, *Stochastic Variational Approach to Quantum-Mechanical Few-Body Problems* (Springer, 1998).
- ⁴⁴C. D. Lin, “Hyperspherical coordinate approach to atomic and other Coulombic three-body systems,” *Phys. Rep.* **257**, 1–83 (1995).
- ⁴⁵J. Avery, *Hyperspherical Harmonics: Applications in Quantum Theory*, *Reidel Texts in the Mathematical Sciences* (Springer Netherlands, 2012).
- ⁴⁶J. Pérez-Ríos, *An Introduction to Cold and Ultracold Chemistry* (Springer International Publishing, 2020).
- ⁴⁷M. J. Elrod and R. J. Saykally, “Many-body effects in intermolecular forces,” *Chem. Rev.* **94**, 1975–1997 (1994).
- ⁴⁸A. M. Reilly and A. Tkatchenko, “van der Waals dispersion interactions in molecular materials: Beyond pairwise additivity,” *Chem. Sci.* **6**, 3289–3301 (2015).
- ⁴⁹N. Moazzen-Ahmadi and A. R. W. McKellar, “Spectroscopy of dimers, trimers and larger clusters of linear molecules,” *Int. Rev. Phys. Chem.* **32**, 611–650 (2013).
- ⁵⁰C. Makrides, J. Hazra, G. B. Pradhan, A. Petrov, B. K. Kendrick, T. González-Lezana, N. Balakrishnan, and S. Kotochigova, “Ultracold chemistry with alkali-metal-rare-earth molecules,” *Phys. Rev. A* **91**, 012708 (2015).
- ⁵¹F. T. Smith, “Generalized angular momentum in many-body collisions,” *Phys. Rev.* **120**, 1058–1069 (1960).
- ⁵²A. J. Dragt, “Classification of three-particle states according to SU 3,” *J. Math. Phys.* **6**, 533–553 (1965).
- ⁵³R. C. Whitten and F. T. Smith, “Symmetric representation for three-body problems. II. Motion in space,” *J. Math. Phys.* **9**, 1103–1113 (1968).
- ⁵⁴U. Kleinekathöfer, K. T. Tang, J. P. Toennies, and C. L. Yiu, “Potentials for some rare gas and alkali-helium systems calculated from the surface integral method,” *Chem. Phys. Lett.* **249**, 257–263 (1996).
- ⁵⁵U. Kleinekathöfer, M. Lewerenz, and M. Mladenović, “Long range binding in alkali-helium pairs,” *Phys. Rev. Lett.* **83**, 4717–4720 (1999).
- ⁵⁶R. A. Aziz, A. R. Janzen, and M. R. Moldover, “Ab initio calculations for helium: A standard for transport property measurements,” *Phys. Rev. Lett.* **74**, 1586–1589 (1995).
- ⁵⁷J. Jiang, J. Mitroy, Y. Cheng, and M. W. J. Bromley, “Effective oscillator strength distributions of spherically symmetric atoms for calculating polarizabilities and long-range atom-atom interactions,” *At. Data Nucl. Data Tables* **101**, 158–186 (2015).
- ⁵⁸F. Maeder and W. Kutzelnigg, “Natural states of interacting systems and their use for the calculation of intermolecular forces,” *Chem. Phys.* **42**, 95–112 (1979).
- ⁵⁹A. Kumar and W. J. Meath, “Pseudo-spectral dipole oscillator strengths and dipole-dipole and triple-dipole dispersion energy coefficients for HF, HCl, HBr, He, Ne, Ar, Kr and Xe,” *Mol. Phys.* **54**, 823–833 (1985).
- ⁶⁰J. Tao, J. P. Perdew, and A. Ruzsinszky, “Long-range van der Waals attraction and alkali-metal lattice constants,” *Phys. Rev. B* **81**, 233102 (2010).
- ⁶¹G. P. Yin, P. Li, and K. T. Tang, “The ground state van der Waals potentials of the strontium dimer and strontium rare-gas complexes,” *J. Chem. Phys.* **132**, 074303 (2010).
- ⁶²H. Partridge, J. R. Stallcop, and E. Levin, “Potential energy curves and transport properties for the interaction of He with other ground-state atoms,” *J. Chem. Phys.* **115**, 6471–6488 (2001).
- ⁶³V. Aquilanti, R. Candori, and F. Pirani, “Molecular beam studies of weak interactions for open-shell systems: The ground and lowest excited states of rare gas oxides,” *J. Chem. Phys.* **89**, 6157–6164 (1988).
- ⁶⁴V. Aquilanti, E. Luzzatti, F. Pirani, and G. G. Volpi, “Molecular beam studies of weak interactions for open-shell systems: The ground and lowest excited states of ArF, KrF, and XeF,” *J. Chem. Phys.* **89**, 6165–6175 (1988).
- ⁶⁵V. P. Singh, *Entropy-Based Parameter Estimation in Hydrology* (Springer Netherlands, Dordrecht, 1998).
- ⁶⁶S. Markose and A. Alentorn, “The generalized extreme value distribution, implied tail index, and option pricing,” *J. Deriv.* **18**, 35–60 (2011).
- ⁶⁷M. P. Langevin, “Une formule fondamentale de théorie cinétique,” *Ann. Chim. Phys.* **5**, 245–288 (1905).
- ⁶⁸I. S. Gradshteyn and I. M. Ryzhik, *Table of Integrals, Series, and Products*, 6th ed. (Academic Press, 2000).
- ⁶⁹J. Pérez-Ríos, “Cold chemistry: A few-body perspective on impurity physics of a single ion in an ultracold bath,” *Mol. Phys.* **119**, e1881637 (2021).